FOR THE RECORD

Inositol phosphate-induced stabilization of inositol 1,3,4,5,6-pentakisphosphate 2-kinase and its role in substrate specificity

Varin Gosein,[1] Ting-Fung Leung,[1] Oren Krajden,[1] and Gregory J. Miller[1,2,3]*

[1]Department of Pharmacology and Therapeutics, McGill University, Montreal, Canada, H3G 1Y6
[2]Groupe de Recherche Axé sur la Structure des Protéines, McGill University, Montréal, Québec H3G 0B1, Canada
[3]Department of Chemistry, The Catholic University of America, Washington, DC, 20064

Received 2 December 2011; Revised 7 February 2012; Accepted 8 February 2012
DOI: 10.1002/pro.2049
Published online 23 February 2012 proteinscience.org

Abstract: Inositol phosphate kinases (IPKs) sequentially phosphorylate inositol phosphates (IPs) on their inositol rings to yield an array of signaling molecules. IPKs must possess the ability to recognize their physiological substrates from among a pool of over 30 cellular IPs that differ in numbers and positions of phosphates. Crystal structures from IPK subfamilies have revealed structural determinants for IP discrimination, which vary considerably between IPKs. However, recent structures of inositol 1,3,4,5,6-pentakisphosphate 2-kinase (IPK1) did not reveal how IPK1 selectively recognizes its physiological substrate, IP5, while excluding others. Here, we report that limited proteolysis has revealed the presence of multiple conformational states in the IPK1 catalytic cycle, with notable protection from protease only in the presence of IP. Further, a 3.1-Å crystal structure of IPK1 bound to ADP in the absence of IP revealed decreased order in residues 110–140 within the N-lobe of the kinase compared with structures in which IP is bound. Using this solution and crystallographic data, we propose a model for recognition of IP substrate by IPK1 wherein phosphate groups at the 4-, 5-, and 6-positions are recognized initially by the C-lobe with subsequent interaction of the 1-position phosphate by Arg130 that stabilizes this residue and the N-lobe. This model explains how IPK1 can be highly specific for a single IP substrate by linking its interactions with substrate phosphate groups to the stabilization of the N- and C-lobes and kinase activation.

Keywords: inositol phosphate; kinase activation; substrate recognition; enzyme specificity

Introduction

Inositol phosphate kinases (IPKs) sequentially phosphorylate inositol phosphates (IPs) on their inositol rings to yield an array of unique signaling molecules with diverse cellular functions.[1,2] Among these functions, IPs are implicated in a variety of diseases such as cancer and diabetes.[3–5] IPKs must discriminate between IPs with different numbers and positions of phosphates to recognize specifically their physiological substrates. Crystal structures from each of the IPK subfamilies have revealed structural

Additional Supporting Information may be found in the online version of this article.

Grant sponsor: Canadian Institutes of Health Research Operating Grant; Grant number: MOP-93687; Grant sponsor: CIHR New Investigator Award; a CIHR Strategic Training Initiative in Chemical Biology.

*Correspondence to: Gregory J. Miller, Department of Chemistry, The Catholic University of America, Washington, DC, 20064. E-mail: millergj@cua.edu

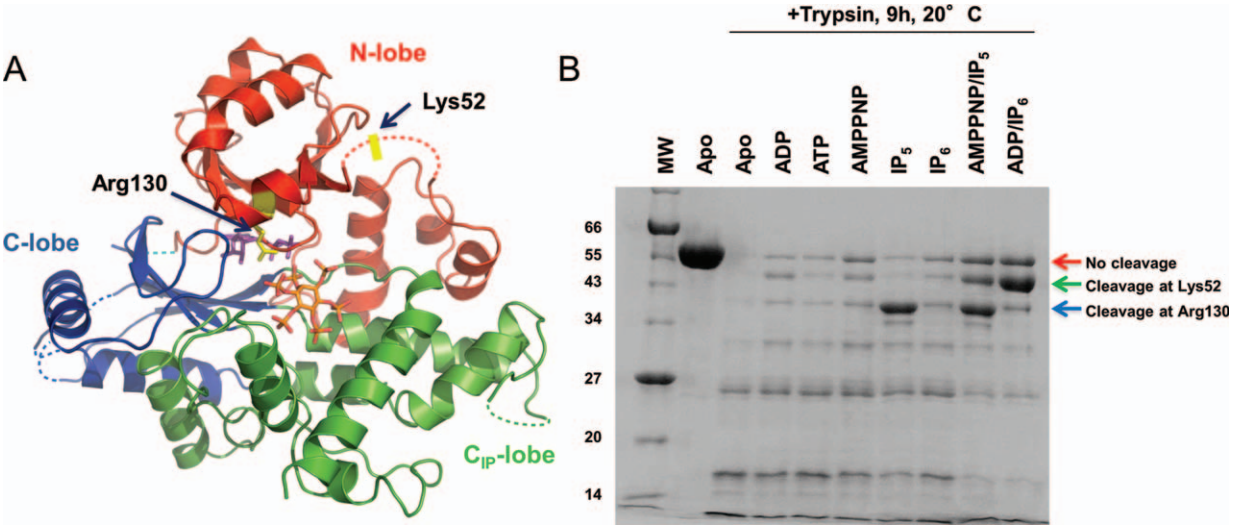

Figure 1. Limited Proteolysis of IPK1. (A) Cartoon representation of product-bound IPK1 depicting overall topology: N-lobe (red), C-lobe (blue), hinge (cyan), C_{IP}-lobe (green) with ADP (purple) and IP_6 (orange); PDB ID: 3UDZ. Dashed lies indicate untraceable regions; (B) IPK1 (55 kDa) was incubated with trypsin in numerous conditions with nucleotides and/or inositides. Two fragments were protected in multiple conditions. N-terminal sequencing identified one fragment to be cleaved after Lys52 (46 kDa) and the other to be cleaved after Arg130 (37 kDa). Both residues are shown in yellow in a (R130, sticks; K52, rectangle).

determinants for IP discrimination, which vary considerably between IPKs. Strict specificity of inositol 1,4,5-trisphosphate 3-kinase (IP_3K) relies upon shape complementarity with the sparsely phosphorylated IP_3 substrate, and it binds to both precisely positioned phosphate and hydroxyl groups.[6] In contrast, the active site of inositol 1,3,4-trisphosphate 5/6-kinase (ITPK1) exhibits little shape complementarity with its varied substrates and its affinity for them is dictated by contacts with phosphates alone, thereby permitting promiscuous substrate recognition.[7] Inositol 1,3,4,5,6-pentakisphosphate 2-kinase (IPK1) is uniquely specific for a single highly phosphorylated IP, inositol 1,3,4,5,6-pentakisphosphate (IP_5), which demands use of a mechanism distinct from those used by IP_3K or ITPK1 to achieve selectivity.

The recently determined crystal structures of IPK1 in its IP substrate- and product-bound forms revealed extensive contacts with phosphate groups of IPs and the mechanism through which the axial 2′ hydroxyl of its substrate is selectively phosphorylated.[8] These four structures are highly similar with no significant differences (RMSD = 0.48 Å) suggesting IPK1 adopts the same conformation regardless of whether it is substrate- or product-bound [Fig. 1(a)]. However, it was not clear from these similar structures how IPK1 recognizes IP_5 while excluding other IPs with similar stereochemistry at the 2′ hydroxyl and phosphate groups. We hypothesized that this selectivity is defined by a previously unrecognized conformational change triggered by binding of an IP with a specific phosphate profile.

Results and Discussion

To confirm the presence of different conformational states in the IPK1 catalytic cycle, we performed limited proteolysis of IPK1 in its free state, bound to nucleotides or to a nucleotide analogue (ATP, ADP, or AMPPNP), inositol phosphate (IP_5 or IP_6), and in ternary complexes (AMPPNP+IP_5 or ADP+IP_6) [Fig. 1(b)]. Trypsin digests were performed at 20°C for 9 h and the resulting proteolytic patterns were compared on SDS gels to detect distinct conformations. Differences in the digestion patterns were evident, indicating that IPK1 adopts a series of conformations in solution. In the apo state, IPK1 is extensively digested to small fragments indicating that free IPK1 is protease labile and suggesting that it is flexible in solution. Nucleotides alone exhibited modest protection of IPK1 from proteolysis but the digestion pattern revealed no protection of stable domains. IP_6 binding also provided little protection from protease. This is in contrast to IP_5, which protected a 37 kDa fragment not protected in the apo state, which is indicative of IP-induced stabilization of IPK1. N-terminal sequencing revealed that this 37 kDa-protected fragment resulted from trypsin cleavage between Arg130 and Val131 while all residues C-terminal to Arg130 remained intact, thereby demonstrating stabilization of the C-lobe of the kinase but not the N-lobe. No differences were reported between the IP_5- and IP_6-bound IPK1 crystal structures, indicating that there are differences in conformational dynamics in different ligand-bound states that may not be detectable in static crystal structures. Finally, we observed synergistic

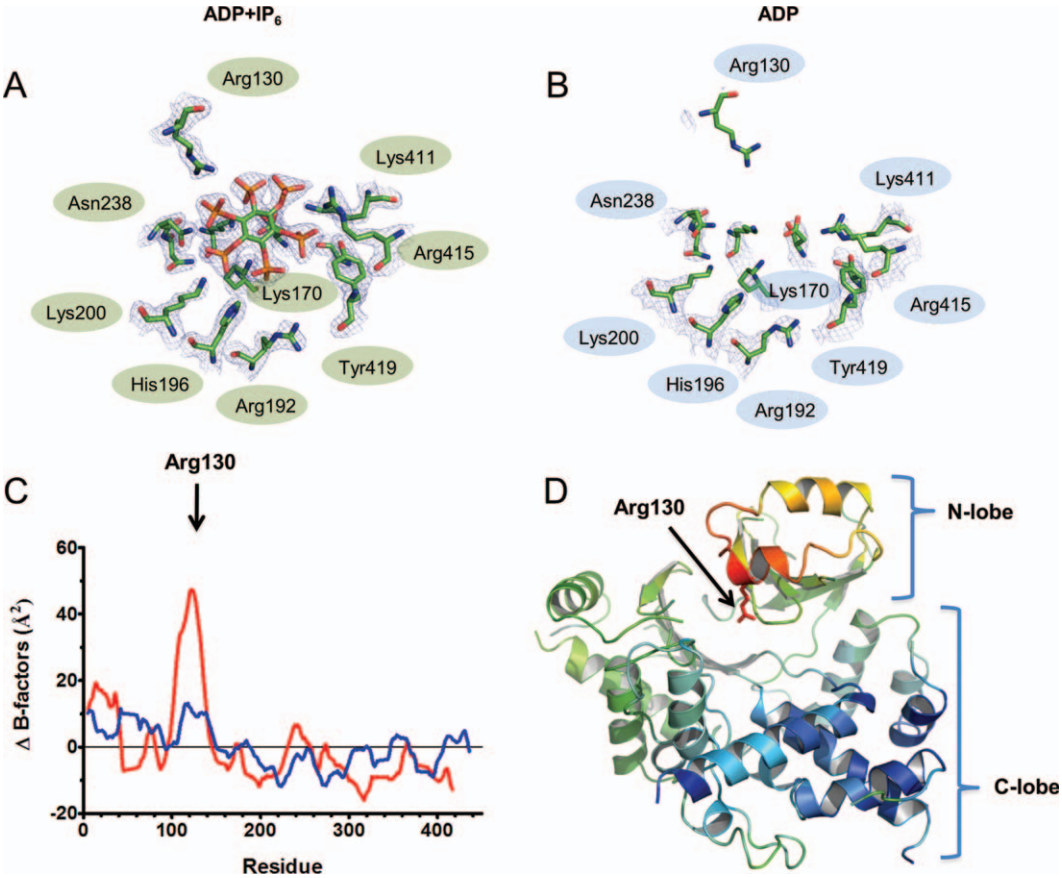

Figure 2. IPK1 exhibits localized disorder of the N-lobe in absence of substrate. Electron density of substrate binding residues ($2F_o - F_c$ (1.8σ)) is shown for crystal structures of IPK1 bound to (A) ADP+IP_6 (B) ADP; (C) Main-chain *B*-factors from the ADP+IP_5 structure were subtracted from the main-chain *B*-factors from the ADP-bound state (Red) and ADP+IP_6 bound state (Blue); (D) Cartoon representation of ADP-bound crystal structure colored by *B*-factors differences between ADP-bound state and ADP+IP_6-bound states. Blue represents no difference while red represents highest differences.

protection in the ternary complexes. Here, when bound also by nucleotides, both IP_5 and IP_6 protected IPK1 from cleavage at Arg130, albeit to different extents. The additional 46-kDa fragment stabilized in the ternary complexes is cleaved by trypsin at Lys52 while the remainder of the protein remains intact, including the site at Arg130. This synergistic protection of Arg130 revealed stabilization of both the N- and the C-lobes of the kinase, which has been reported to be a critical step in kinase activation.[9–11]

To further explore the conformational changes IPK1 undergoes during IP binding, we determined the nucleotide-bound structure of IPK1 in the absence and presence of its IP substrate and compared features of these structures to identify the mechanism by which IPK1 transitions into its catalytically active state.

Here, we present the 3.1 Å crystal structure of IPK1 bound to ADP in the absence of IP (Table 1). Overall, this structure is very similar to the previously solved crystal structures of IP-bound IPK1 with and without nucleotides and our own structure of IPK1 bound to ADP+IP6. There are no gross conformational differences between the IP-bound and free structures in the C-lobe (RMSD = 0.40 Å) of the kinase and no differences in positions or *B*-factors of the residues that bind the 4-, 5-, and 6-phosphates of the IP. In this structure, IP-binding residues, including Lys411, Arg415, Tyr419, Lys170, Arg192, His196, Lys200, and Asn238, are all positioned as they are in the IP-bound states [Fig. 2(a)]. These residues are likely held in place by water molecules that create a network of interactions in the absence of IP, but this supposition is speculative as the resolution of the structure (3.1 Å) was too low to confirm positions of solvent molecules. Between the ADP-bound state and all IP-bound structures, there is a notable difference in the orientation of the residue that interacts with the 1-phosphate of the IP [Fig. 2(a,b)]. The side chain for Arg130 cannot be modeled in the ADP-alone state, suggesting that this residue becomes ordered only upon occupancy of the active site by the correct substrate.

To identify regions of decreased order in the ADP-bound state, we compared *B*-factors among ADP+IP_6-bound-, ADP+IP_5-bound- and the ADP-bound-IPK1 structures [Fig. 2(c)]. Only modest

Table I. *Data Collection and Refinement Statistics (Molecular Replacement with PDB ID: 2XAM)*

	ADP (PDB: 3UDS)	ADP+IP6 (PDB: 3UDT)	ADP+IP5 (PDB: 3UDZ)
Data collection			
Space group	P1	P1	P1
Cell dimensions			
a, *b*, *c* (Å)	58.29, 59.88, 82.91	59.06, 59.39, 82.75	59.36, 59.91, 83.14
α, β, γ (°)	83.40, 89.40, 65.30	89.84, 82.58, 63.36	90.02, 97.04, 116.81
Resolution (Å)	50.00–3.10 (3.29–3.10)*	50.00–2.50 (2.58–2.50)	50.00–3.10 (3.26–3.10)
R_{merge}	0.061 (0.134)	0.084 (0.152)	0.132 (0.218)
$I/\sigma I$	15.1 (7.7)	39.1 (15.8)	16.7 (7.0)
Completeness (%)	95.15 (90)	94.5 (91)	96.4 (95)
Redundancy (%)	3.9 (3.9)	3.7 (3.7)	3.9 (4.0)
Refinement			
Resolution (Å)	42.82–3.10	41.43–2.50	44.62–3.10
No. reflections	17,449	32,523	17,694
R_{work}/R_{free}	0.2370/0.3119	0.1890/0.2595	0.2098/0.2762
No. atoms	5,796	6,761	6,267
Protein	5,740	6,169	6,145
Ligand/ion	56	131	122
Water	0	461	0
B-factors (Å^2)			
Protein	64.31	35.28	26.26
Ligand/ion	65.12	27.81	36.02
Water	0	32.50	0
R.m.s. deviations			
Bond lengths (Å)	0.013	0.022	0.011
Bond angles (°)	1.319	1.229	1.287

* One single crystal used for each data collection. *Values in parentheses are for highest-resolution shell.

differences were detectable between the ADP+IP_5- and ADP+IP_6-bound states (blue line), but compared with either of these structures, there were substantial localized increases in *B*-factors in the ADP-bound state (red line). Specifically, marked differences in *B*-factors were observed for residues 110–140 in the N-lobe of the kinase when the ADP+IP_6 and the ADP-bound structures were compared. Consistent with the limited proteolysis in solution where IPK1 is cleaved at Arg130 in the absence of IP, we see a destabilization of the region surrounding Arg130 in the IP-free crystal structure, which appears to be shared with much of the N-lobe of the kinase [Fig. 2(d)].

Our limited proteolysis and IP-free crystal structure indicate that IPK1 adopts multiple conformational states not appreciated from previous crystal structures. Here, the decreased order in the crystal structure is consistent with the protease sensitivity in solution supporting our use of the crystal structure to propose dynamics of the N-lobe of the kinase in the absence of IP substrate. The different extents of protease protection in these states suggest that conformational dynamics may play a more significant role in the IPK1 catalytic cycle than previously thought.

Consistent with these observations, we propose a model for recognition of IP substrate by IPK1 wherein phosphate groups at the 4-, 5- and 6-positions are required for initial recognition of IP_5 by the residues Lys411, Arg415, Tyr419, Lys170, Arg192, His196, Lys200, and Asn238, which are poised for binding IP_5 in the IP-free state [Fig. 3(a)]. Subsequently, interaction of a 1-position phosphate with Arg130 stabilizes this residue and the N-lobe. In this 2-step model for substrate recognition and activation, contacts at the 4-, 5-, and 6- positions are needed for initial recognition and the 1-phosphate is required for IPK1 subsequently to adopt an active conformation. In this model, the 4-, 5-, and 6- phosphates share the role for mediating initial substrate contact with the enzyme, while the 1-phosphate plays the subsequent, but critical role of stabilizing the N-lobe of the kinase, an essential step for kinase activation [Fig. 3(b)]. This model—including the critical role of the 1-phosphate—is consistent with the report that IPK1 exhibits some activity toward inositol 1,3,4,6-tetrakisphosphate but no activity towards inositol 3,4,5,6-tetrakisphosphate, which lacks the 1-phosphate.[12]

Knockout of the IPK1 gene in mice is embryonic lethal[13] and RNAi of IPK1 in zebrafish exhibit developmental defects[14] which suggest an important physiological role for IPK1. Characterizing the mechanism IPK1 uses for substrate recognition opens up new avenues for selectively targeting IPK1 as the similarity among IP substrates has previously hindered the development of specific inhibitors for IPKs.

Materials and Methods

Protein expression and purification

Arabidopsis thaliana IPK1 (IPK1) was previously cloned into a pET28a vector containing a 6xHis tag

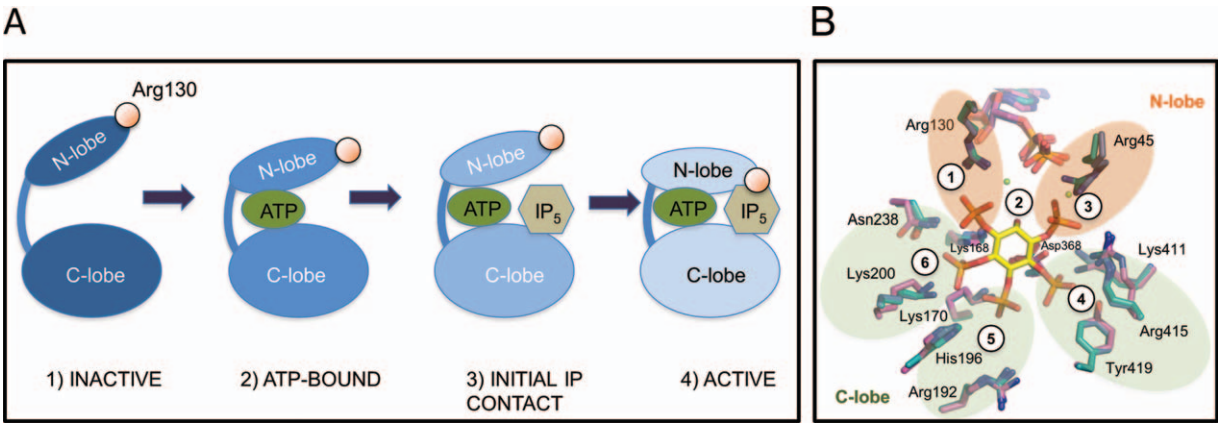

Figure 3. Proposed Model of IPK1 Activation. (A) In the inactive state, IPK1 remains an open "clamshell" (1) which closes slightly upon binding of ATP (2). IP_5 is then initially recognized at the 4-, 5- and 6- positions (3). Finally, with IP_5 bound, interactions between Arg130 and 1-phosphate stabilize the N-lobe of the kinase into the active state; (B) Two classes of interactions with IP substrate are necessary for IPK1 activity. The 4-, 5- and 6- positions of IP_5 are required for initial recognition, while the 1- and 3- positions are required for N-lobe stabilization.

and expressed in Bl-21 AI cells (Invitrogen). Cells were grown in Terrific broth with kanamycin at 37°C to an $OD_{600} = 1.5$ and protein over-expression was induced with 0.5 m*M* IPTG and 0.1% L-arabinose at 18°C for 20 h. Cells were harvested at 5000*g* and were lysed for 1 h using a sonicator in 10 m*M* Tris-HCl pH 8, 250 m*M* NaCl and 50% glycerol. Supernatant was separated from lysate using centrifugation. The supernatant was then diluted 5-fold using 20 m*M* Tris-HCl pH 8 and 500 m*M* NaCl and then 25 m*M* imidazole was added. IPK1 was purified by applying the diluted supernatant to an Ni-NTA column followed by washing with 20-column volumes of 50 m*M* KPO_4 pH 8.0, 800 m*M* NaCl, 1% Triton X-100, 1.7 m*M* β-mercaptoethanol. Protein was eluted using 10-column volumes of 250 m*M* imidazole in 20 m*M* Tris-HCl pH 8.0, 300 m*M* NaCl buffer and subsequently dialyzed into 50 m*M* Tris-HCl pH 8.0, 50 m*M* NaCl, and 1 m*M* DTT. Next, the protein was applied to a 5 mL Heparin SP FF column. The column was washed with 10-column volumes of dialysis buffer and IPK1 was eluted over an increasing NaCl concentration gradient. Fractions containing purified protein were analyzed by SDS-PAGE and pooled accordingly. Finally, the pooled sample was applied to a S-300 Sephacryl gel filtration column equilibrated in 50 m*M* Tris-HCl pH 8.0, 150 m*M* NaCl, and 2.5 m*M* DTT. Fractions containing IPK1 were analyzed by SDS-PAGE and pooled accordingly. The protein was concentrated to 20 mg/mL and stored at 4°C.

Protein crystallization

All crystals grew at 20°C within 6–72 h using the sitting-drop vapor-diffusion method. All ligand solutions were pH 8 prior to incubating with protein for 30 min at 4°C. IP_6 was purchased from Sigma-Alrich. IP_5 was purchased from Cayman Chemical Company. IPK1 (5 mg/mL) crystallized with 5 m*M* ADP/IP_6/$MgCl_2$ in 0.08*M* MES pH 6.5, 19.85% PEG 3000, 0.17*M* NaCl, 2.35% benzamidine HCl. For the substrate-bound state, IPK1 (5 mg/mL) crystallized with 2 m*M* ADP/IP_5, 4 m*M* $MgCl_2$ in 0.09*M* MES pH = 6.5, 18% PEG4000, 0.54*M* NaCl, 0.01*M* Trimethylamine HCl. For the ADP-only bound state, IPK1 (10 mg/mL) crystallized with 5 m*M* ADP/$MgCl_2$ in 0.18*M* $CaCl_2$, 0.1*M* Tris-HCl pH 8.0, 18.18% PEG6000, 0.01*M* TCEP.

Data collection

X-ray diffraction data for all complexes were collected on a Rigaku MicroMax-007 HF microfocus X-ray generator fitted with Varimax X-ray optics and a Saturn 944+ CCD detector. All data were measured under cryogenic conditions, cryoprotected with reservoir solution including 5–10% PEG400, and processed with HKL2000 software.[15]

Structure determination and refinement

Diffraction data was analyzed and processed with HKL2000 software and refined with Phenix[16] and Coot.[17] Molecular replacement was performed with PDB ID: 2XAM. All model images were created using PyMol (DeLano Scientific).

Limited proteolysis

Limited proteolysis of IPK1 was performed in 50 m*M* Tris-HCl pH 8.0, 150 m*M* NaCl, and 2.5 m*M* DTT buffer in separate 1.5-mL microfuge tubes. Totally, 80 μg of IPK1 was incubated with 2 m*M* $MgCl_2$, 2 m*M* of nucleotide (ATP, ADP, AMPPNP), and/or 2 m*M* of inositol phosphate (IP_5 or IP_6) for 20 min at 4°C. Totally, 0.08 μg of trypsin was added resulting in a final volume of 200 μL. The reactions were incubated at 20°C and 50 μL samples were taken at 1, 5, 9, and 16 h. Samples were analyzed

by SDS-PAGE and stained with Coomassie blue. For N-terminal sequencing, a duplicate gel was run and bands were transferred to a PVDF membrane. The blot was submitted to the Sheldon Biotechnology Centre (McGill University, Montreal, QC) for N-terminal sequencing of the fragments.

B-*factor analysis*

B-factors were extracted from PDB files using StrucTools (http://helixweb.nih.gov/structbio/basic.html). Main chain *B*-factors from the ADP+IP_5 structure were subtracted from the ADP structure and ADP+IP_6 structure to provide a baseline for *B*-factor comparison between ADP and ADP+IP_6 complexes. Calculated *B*-factor differences were plotted using GraphPad Prism (GraphPad Software). The curves were smoothed by averaging the calculated *B*-factor differences for each residue with those of its four neighboring residues.

Acknowledgments

The authors thank C.A. Brearley (University of East Anglia) for his gift of the AtIPK1-pET28 vector, J. Hu (McGill University) for performing N-terminal sequencing, D. Rodionov (McGill University) for assistance in crystal diffraction and A. Coventry for critical reading of the manuscript. O.K. expressed and purified IPK1, T-F.L. optimized IPK1 purification, grew initial IPK1 crystals, and collected X-ray diffraction data, V.G. purified IPK1, optimized the IPK1 crystals, collected X-ray diffraction data, analyzed data, and prepared the manuscript, and G.J.M. coordinated the experiments, analyzed data, and prepared the manuscript.

References

1. Majerus PW (1992) Inositol phosphate biochemistry. Annu Rev Biochem 61:225–250.
2. Shears SB (1998) The versatility of inositol phosphates as cellular signals. Biochim Biophys Acta 1436:49–67.
3. Piccolo E, Vignati S, Maffucci T, Innominato PF, Riley AM, Potter BV, Pandolfi PP, Broggini M, Iacobelli S, Innocenti P, Falasca M (2004) Inositol pentakisphosphate promotes apoptosis through the PI 3-K/Akt pathway. Oncogene 23:1754–1765.
4. Irvine RF (2005) Inositide evolution—towards turtle domination? J Physiol 566:295–300.
5. Shi Y, Azab AN, Thompson MN, Greenberg ML (2006) Inositol phosphates and phosphoinositides in health and disease. Subcell Biochem 39:265–292.
6. Gonzalez B, Schell MJ, Letcher AJ, Veprintsev DB, Irvine RF, Williams RL (2004) Structure of a human inositol 1,4,5-trisphosphate 3-kinase: substrate binding reveals why it is not a phosphoinositide 3-kinase. Mol Cell 15:689–701.
7. Miller GJ, Wilson MP, Majerus PW, Hurley JH (2005) Specificity determinants in inositol polyphosphate synthesis: crystal structure of inositol 1,3,4-trisphosphate 5/6-kinase. Mol Cell 18:201–212.
8. Gonzalez B, Banos-Sanz JI, Villate M, Brearley CA, Sanz-Aparicio J (2010) Inositol 1,3,4,5,6-pentakisphosphate 2-kinase is a distant IPK member with a singular inositide binding site for axial 2-OH recognition. Proc Natl Acad Sci USA 107:9608–9613.
9. Knighton DR, Zheng JH, Ten Eyck LF, Xuong NH, Taylor SS, Sowadski JM (1991) Structure of a peptide inhibitor bound to the catalytic subunit of cyclic adenosine monophosphate-dependent protein kinase. Science 253:414–420.
10. Sicheri F, Moarefi I, Kuriyan J (1997) Crystal structure of the Src family tyrosine kinase Hck. Nature 385: 602–609.
11. Ozkirimli E, Post CB (2006) Src kinase activation: a switched electrostatic network. Protein Sci 15: 1051–1062.
12. Sweetman D, Johnson S, Caddick SE, Hanke DE, Brearley CA (2006) Characterization of an Arabidopsis inositol 1,3,4,5,6-pentakisphosphate 2-kinase (AtIPK1). Biochem J 394:95–103.
13. Verbsky J, Lavine K, Majerus PW (2005) Disruption of the mouse inositol 1,3,4,5,6-pentakisphosphate 2-kinase gene, associated lethality, and tissue distribution of 2-kinase expression. Proc Natl Acad Sci USA 102: 8448–8453.
14. Sarmah B, Latimer AJ, Appel B, Wente SR (2005) Inositol polyphosphates regulate zebrafish left-right asymmetry. Dev Cell 9:133–145.
15. Otwinowski Z, Minor W (1997) Processing of X-ray diffraction data collected in oscillation mode. Method Enzymol 276:307–326.
16. Adams PD, Afonine PV, Bunkoczi G, Chen VB, Davis IW, Echols N, Headd JJ, Hung LW, Kapral GJ, Grosse-Kunstleve RW, McCoy AJ, Moriarty NW, Oeffner R, Read RJ, Richardson DC, Richardson JS, Terwilliger TC, Zwart PH (2010) PHENIX: a comprehensive Python-based system for macromolecular structure solution. Acta Crystallogr D Biol Crystallogr 66:213–221.
17. Emsley P, Cowtan K (2004) Coot: model-building tools for molecular graphics. Acta Crystallogr D Biol Crystallogr 60:2126–2132.